

Cite this: DOI: 10.1039/c0an00907e

www.rsc.org/analyst

PAPER

## Development of a fluorescent method for detecting the onset of coagulation in human plasma on microstructured lateral flow platforms†

Magdalena M. Dudek,<sup>a</sup> Nigel J. Kent,<sup>b</sup> Pan Gu,<sup>c</sup> Z. Hugh Fan<sup>c</sup> and Anthony J. Killard<sup>\*ad</sup>

Received 12th November 2010, Accepted 11th January 2011

DOI: 10.1039/c0an00907e

Microfluidic devices and microsystems have been used to develop blood coagulation monitoring devices for point of care diagnostic use. However, many of them suffer from inherent variability and imprecision, partly due to the fact that they only detect changes in bulk clotting properties and do not reflect the microscopic nature of blood coagulation. This work demonstrates microstructured lateral flow platforms used in combination with fluorescently labelled fibrinogen to detect microscopic clot formation. Plasma samples applied to platforms modified with coagulation activation reagents and fluorescent fibrinogen produced changes in fluorescence intensity due to incorporation of the fluorophore into the forming microclots. It was found that the change in the distribution of the fluorescence within the sample over time was an excellent predictor of the onset of coagulation, which could be used to determine the clotting time. The impact of various assay parameters was optimised and the assay was shown to be capable of measuring the effect of heparin concentration on blood clotting time from 0 to 1.5 U mL<sup>-1</sup>.

### Introduction

The monitoring of a person's blood clotting status is critical in identifying coagulation disorders and monitoring the effect of anticoagulant or procoagulant drug therapies for a wide variety of conditions and associated medical procedures. For these reasons, tests for measuring blood coagulation are some of the most widely used in the clinical environment. They typically measure how long it takes for an individual's blood to clot when clotting is activated in a controlled and reproducible manner. Several distinct tests are available which activate coagulation *via* particular pathways and they give different information on the individual's clotting status.<sup>1</sup> However, in general, all these tests measure the same parameter which is the conversion of the liquid blood to a gel-like solid. This is the end-point of coagulation and is due to the conversion of soluble fibrinogen into an insoluble fibrin network. Thus, most tests detect this change in bulk viscosity which accompanies this process and the time it takes to occur.<sup>2</sup> However, the available techniques for monitoring this change in bulk viscosity are inherently imprecise. This is due, in

part, to the inherent variability in the constitution of any given blood sample and to the very nature of the clotting process.<sup>3–8</sup>

The kinetics of coagulation have been studied and have been defined as a stochastic process with significant inherent randomness.<sup>9</sup> Coagulation is a cascade with multiple steps with associated positive feedback loops. The process requires an initiation step which triggers this sequence of events. When performed *in vitro*, the precise time and location of this event is difficult to ascertain. Indeed, triggering of coagulation may take place in multiple locations at slightly different times. Thus, the bulk change in viscosity reflects the macroscopic outcome of this unpredictable process and results in significant variability<sup>10</sup> typically in excess of 10% RSD. The development of techniques that take into account the spatial and temporal changes in viscosity could significantly enhance the quality and utility of this measurement process.

Point of care assay devices and diagnostics are being revolutionised by emerging materials and technologies such as microsystems and microfluidics. The ability to control the interaction of biological samples with assay reagents in a controlled and reproducible manner in a miniaturised format allows for low volume, rapid testing with minimal intervention of a user.<sup>11</sup> The use of processing techniques which create devices with excellent reproducibility and defined surface chemistry properties has been essential for such devices. These properties define how the sample interacts with the device platform and allows precise control of fluid movement. Capillary force has been used extensively in lab-on-a-chip systems to induce such movement and has typically been driven by interfacial forces at a fluid/capillary boundary.<sup>12,13</sup> However, such configurations can have disadvantages such as

<sup>a</sup>Biomedical Diagnostics Institute, National Centre for Sensor Research, Dublin City University, Dublin, 9, Ireland. E-mail: tony.killard@uwe.ac.uk

<sup>b</sup>The Biomedical Devices and Assistive Technology Research Group, College of Engineering and Built Environment, Dublin Institute of Technology, Bolton St, Dublin, 1, Ireland

<sup>c</sup>Departments of Mechanical & Aerospace Engineering and Biomedical Engineering, University of Florida, Gainesville, Florida, 32611-6250, USA

<sup>d</sup>Department of Applied Sciences, University of the West of England, Coldharbour Lane, Bristol, BS16 1QY, UK

† Electronic supplementary information (ESI) available. See DOI: 10.1039/c0an00907e

the low surface area-to-volume ratio which reduces the efficiency of interaction between immobilised reagents and the sample under laminar flow conditions.<sup>14</sup> This also affects the efficiency of the capillary pulling force. Other techniques for inducing capillary flow on such platforms include using arrays of micropillars which individually induce a capillary force, and in concert create a uniform and reproducible capillary force along a lateral flow pathway. Several efforts using this technique have been reported.<sup>14–18</sup> Many such systems are replacing less reliable materials such as nitrocellulose in lateral flow bioassays. Additional material properties such as optical transparency and low fluorescence make them suitable in combination with optical and fluorescence transduction. Materials such as glass are excellent for prototyping purposes and other emerging materials such as the cyclic polyolefins have excellent processability and optical characteristics for device mass production.<sup>19–21</sup>

In this work, a technique was developed to identify the onset of coagulation at the microscopic level, taking into account both the spatial and temporal changes involved. This was achieved by the incorporation of a fluorescent marker within the nascent clot and monitoring its distribution over time. It was found that the change in this distribution was closely correlative with the onset of clotting as evidenced by the formation of fibrin fibres when performed on microstructured surfaces made from either plastics or glass. The change in distribution of the label could be enhanced and optimised with deposition of coagulation reagents and the location for monitoring fluorescence. The assay and platform were shown to be capable of measuring the effect of an anti-coagulant drug on sample clotting time.

## Experimental

Development of a fluorescent assay for the detection of clot formation was investigated on two microstructured substrates; one polymer and one glass. The polymeric platform (Fig. 1a) was composed of cyclic polyolefin (Zeonor) and was fabricated *via* injection molding (4Castchip® model B2.2, Åmic BV, Uppsala, Sweden) forming micropillar projections of 65–70 µm in height, top diameter *ca.* 50 µm, base diameter *ca.* 70 µm, distance between the centres of the pillars in a row of 85 µm, and distance between the centres of the pillars in a column of 185 µm. The second platform was made from glass and was fabricated using conventional photolithography and chemical etching (Fig. 1b). The device consisted of 2 mm wide channels and each channel contained numerous ellipse-shaped micropillars. The major diameter of these pillars was 50 µm and the minor diameter was 30 µm with the between-pillar spacing of 50 µm. Micropillar platforms were modified by deposition of activated partial thromboplastin time (aPTT) clot activating reagents.

A 1.35 µL aliquot of a stock solution of human fibrinogen labelled with Alexa Fluor 488 (Molecular Probes, F-13191) was added to 15 µL of citrated control plasma (HemosIL, Instrumentation Laboratory B.V., Netherlands). 15 µL of 0.025 M CaCl<sub>2</sub> solution (Stago Diagnostica) was then added to reverse the effect of citrate and allow clotting. Immediately after addition of Ca<sup>2+</sup> ions, 25 µL of a test mixture was applied to an aPTT-coated test chip and the measurement was started. Blank controls were prepared by replacing CaCl<sub>2</sub> with NH<sub>4</sub>Cl in order to avoid

recalcification, prevent clotting and maintain the dilution factor and ionic strength.

Clot formation was observed using bright light and fluorescence microscopy. Measurements were performed using an optical system (Fig. 1c) consisting of a CCD camera (Hamamatsu Orca ER) attached to an Olympus IX81 fluorescent microscope equipped with a climate chamber and heating block and a motorised stage. Fluorescence signals were monitored using the following settings: magnification: 10×, excitation at 488 nm and emission at 519 nm, exposure time: 21 ms. The autofocus and the brightness auto-adjustment functions were switched off at all times. Experiments were performed in a dark room at 37 °C.

An area of the micropillar platforms of approx. 650 × 820 µm was imaged every 10 s for up to 1500 s (Fig. 1d). Each image was converted to an array of 1360 × 1024 pixels ( $N > 1.39 \times 10^6$ ), each one outputting a value of fluorescence intensity (Fig. 1e). Each frame was output as an .avi file to a LabView interface which automated calculation of the mean fluorescence and standard deviation (SD) for each frame. Change in the absolute fluorescence signal was monitored. The change in the distribution of the label in the monitored area was also assessed using measurements of SD of the averaged fluorescence signal. The recorded data were also subject to visual analysis, where necessary. The maximum fluorescence signal detection was set according to the optical limitations of the microscope, while the minimum level of fluorescence signal detected by the camera was varied from 0 to 70 arbitrary fluorescence units (f.u.) in order to determine an optimum setting for clotting time (CT) determination in normal clotting and heparinised control plasmas. The effect of heparin concentration on the fluorescent profiles was investigated by spiking the citrated platelet poor plasma with unfractionated heparin (Sigma) at concentrations of 0–2 U mL<sup>-1</sup> according to manufacturer's data.

Three detection areas were investigated along the lateral flow platform surface at three locations along the 20 mm flow path in order to select an area that would reflect the onset of clotting in the most reliable way (Fig. 1a).

The effect of evaporation of a standard clotting sample consisting of plasma and CaCl<sub>2</sub> at a 1 : 1 ratio supplemented with fluorescently labelled fibrinogen (total volume 25 µL) and applied to the microfluidic platform modified with the aPTT-SP reagent was investigated by measuring the percentage loss of a sample mass over a period of 38 min using a standard laboratory balance.

Following on from the establishment of the assay principle, more detailed assay optimisation was undertaken. Variables including aPTT reagent type and volume were optimised with the aim of establishing clear and reproducible fluorescence clotting profiles from which to extract CTs which could be modified by heparin levels.

## Results and discussion

### Investigation of the clot formation and localisation principle

The nature of the clot formation and localisation phenomenon was initially explored on a microstructured surface composed of cyclic polyolefin, fabricated by injection moulding. This device

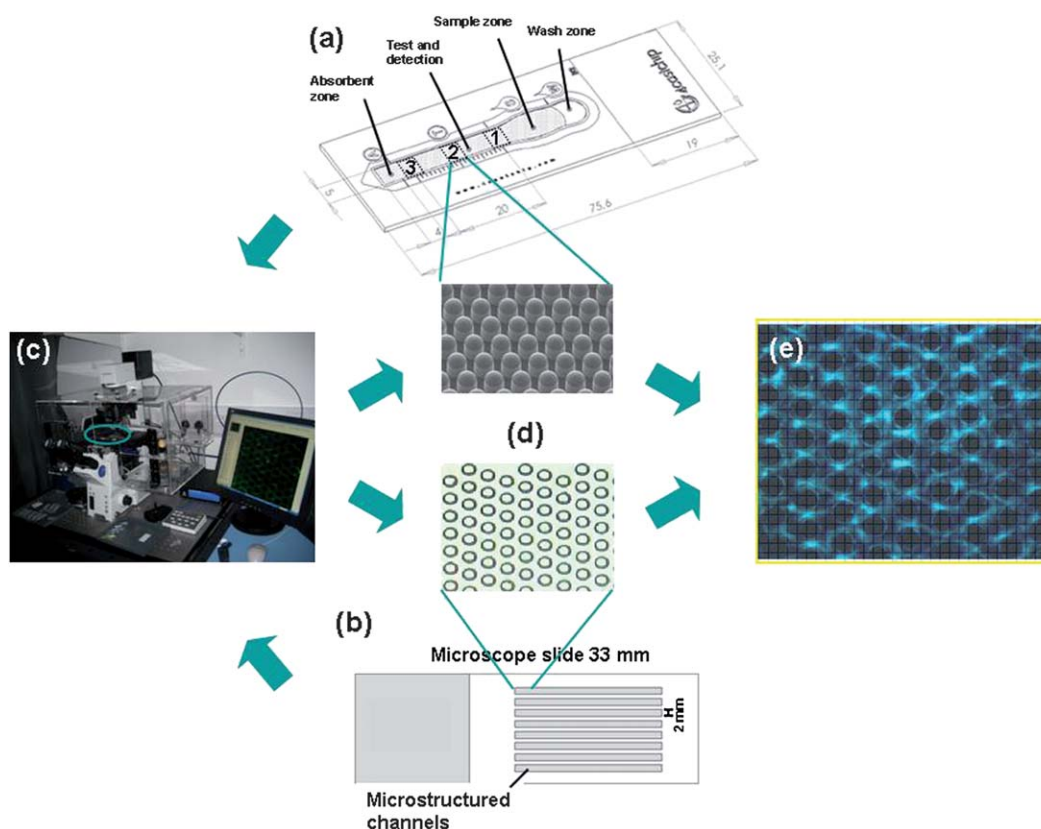


**Fig. 1** Experimental setup for development of the fluorescent lateral flow assay. (a) Polymeric platforms made from cyclic polyolefin with a lateral flow zone composed of micropillars of 65–70  $\mu\text{m}$  in height, top diameter *ca.* 50  $\mu\text{m}$ , base diameter *ca.* 70  $\mu\text{m}$ , distance between the centres of the pillars in a row of 85  $\mu\text{m}$ , and distance between the centres of the pillars in a column of 185  $\mu\text{m}$  and (b) microfabricated glass substrate with 2 mm wide channels, each channel containing ellipse-shaped micropillars of major diameter 50  $\mu\text{m}$  and a minor diameter of 30  $\mu\text{m}$  with the between-pillar spacing of 50  $\mu\text{m}$ . Platforms were modified with deposited clotting reagents and placed in a fluorescence microscope with CCD camera (c). Following addition of blood sample to the platforms, the fluorescence response was monitored in an area of the platforms 650  $\times$  820  $\mu\text{m}$  (d). The imaged area was captured every 10 s and converted to an array of light intensity values (e) and output to a video image file which was processed by a LabView interface.

had been patterned into a lateral flow arrangement (Fig. 1a). Initially, changes in fluorescence were monitored in the centre of the test channel (area 2).

A conjugate of human fibrinogen labelled with Alexa Fluor 488 was used in the assay at a concentration of 5% of normal fibrinogen content in plasma. There was no action required to release a fluorescent signal. In the presence of thrombin the soluble fibrinogen was converted into insoluble fluorescently labelled fibrin. In essence, the labelled fibrin then competes for unlabelled fibrin for incorporation into the forming clot allowing its optical fluorescent localisation. Additionally, binding of the labelled fibrin to the GPIIb-IIa receptor on activated platelets could take place which would supplement the process of fibrin incorporation into a clot. To assess the potential of the fluorescent label to be used to detect clot formation *in vitro*, a plasma test sample was externally recalcified and supplemented with the fluorescently labelled fibrinogen. A sample was applied to a microfluidic chip that had previously been modified by drying aPTT-SP reagent onto the surface. Passage of the liquid sample would lead to solubilisation and reconstitution of the reagent which would then bring about accelerated clotting.

It was found that the sample advanced along the device channel in a highly controlled and reproducible fashion with an initially uniform distribution of the dye. When analysed by light

microscopy, immediately after addition of sample, the mixture was homogeneous (Fig. 2a). However, after 10 min, strands which were believed to be fibrin fibres could be seen gathering around and between the micropillars (Fig. 2b). When analysed using fluorescent microscopy, initially, there was an even distribution of fluorophore with relatively low average background intensity (Fig. 2c). However, following clotting, patches of more intense fluorescence in a pattern similar to that seen for the fibrin fibres under light microscopy could be seen (Fig. 2d). It could also be seen that there was a decrease in fluorescence in areas immediately adjacent to the areas of more intense clot formation, which may be due to the concentration of the labelled fibrinogen within the loci of forming clots.

The concentration of the fluorescently labelled fibrinogen and its distribution along the channel appeared to be changing in a time-dependent manner. Appearance of the highly fluorescing formations could be observed after approx. 300 s (Fig. 2d), which corresponded to the time needed for fibrin fibre formation as observed visually by light microscopy (Fig. 2b). Therefore, the timing of the localisation of clot formation as seen with fluorescence could form the basis of a means of defining an assay CT.

Plasma samples were spiked with a range of heparin concentrations (0–1  $\text{U mL}^{-1}$ ) in order to obtain samples with prolonged CTs (Fig. 3). The change in the average fluorescence over time

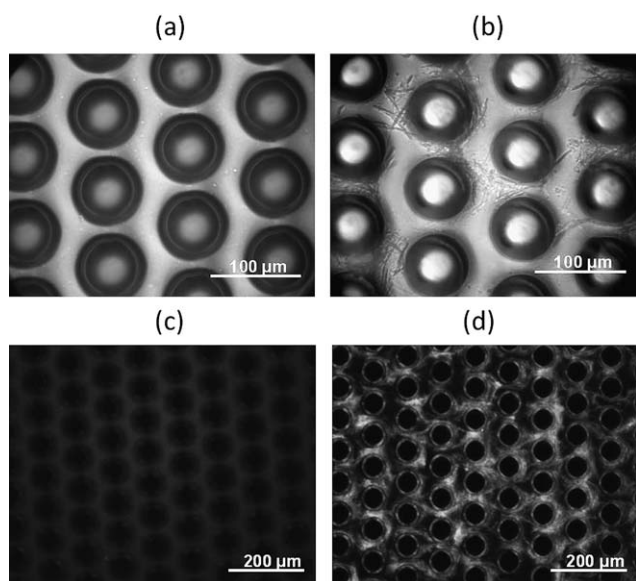


**Fig. 2** Images of recalcified plasma sample supplemented with fluorescently labelled fibrinogen and tested in aPTT reagent-coated (aPTT-SP) lateral flow platforms captured using (a) bright light microscopy, 20 $\times$ , at 5 s, (b) bright light microscopy, 20 $\times$ , at 10 min, (c) fluorescence microscopy, 10 $\times$ , at 5 s and (d) fluorescence microscopy, 10 $\times$ , at 10 min.

was monitored at the centre of the lateral flow device. All samples showed some initial increase in fluorescence intensity, due to the influx of label to the area as it passed down the channel. At some point, however, there was an actual decrease in fluorescence intensity, followed once again by a gradual rise. The point at which this decrease occurred appeared to correlate with the concentration of heparin used, rising from approx. 130 s at 0 U mL<sup>-1</sup> to approx. 220 s for 1 U mL<sup>-1</sup>. However, the profiles generated were not very well defined, particularly at 1 U mL<sup>-1</sup> in which the change in the profile was difficult to interpret. Thus, alternative methods of correlating clotting with changes in fluorescence were investigated.

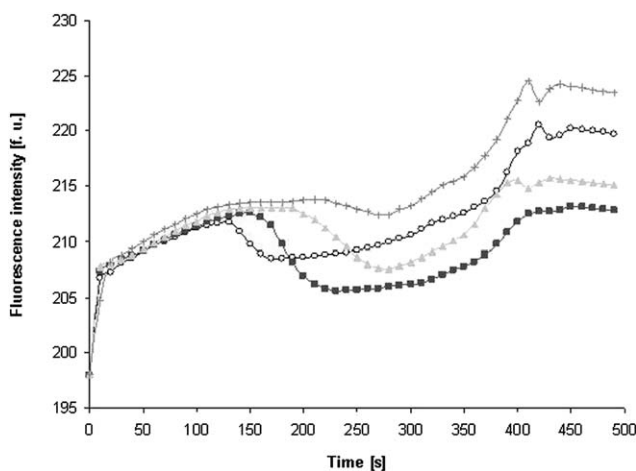


**Fig. 3** Change in mean fluorescence intensity with time measured for fluorescent label-supplemented plasma samples spiked with 0 (circles), 0.25 (squares), 0.5 (triangles) and 1 (crosses) U mL<sup>-1</sup> of heparin tested in aPTT-SP-coated microfluidic channels.

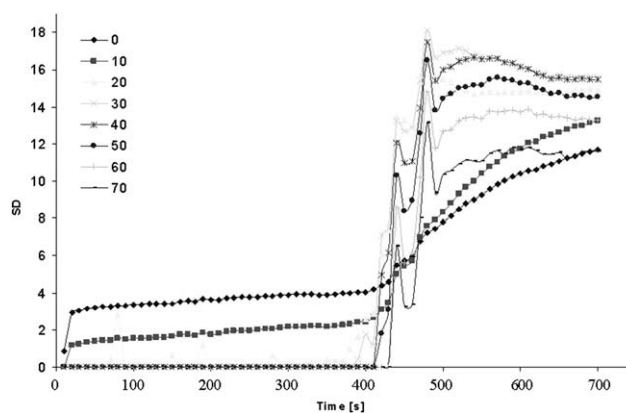
Although it did not appear reliable to extract the CT values from the total change in fluorescence intensity, visual observation had suggested that, as well as changes in the average fluorescence, the localised redistribution of the label within a specific area might also be changing in a time-dependent manner. Therefore, the fluorescence standard deviation (SD) of the monitored zone was assessed.

Fig. 4 shows the change in SD of the fluorescence over time obtained for 0.25 U mL<sup>-1</sup> of heparin in plasma with the fluorescence background detection set between 0 and 70 f.u. The shapes of the profiles obtained for this sample were shown to be highly dependent on the background fluorescence setting. Since all data points in the monitored area were included in the SD measurement, even low signal areas such as the micropillar surface were included in the SD calculation. Increasing the background cut off resulted in the elimination of the low signal regions within the monitored area (most likely coming from the areas of micropillars) and thus lower SD values were obtained. Thus, below 30 f.u., initial SD values were greater than zero, being between 3 and 4 for 0 f.u. and between 2 and 3 SD for 10 f.u. However, above 30 f.u., little or no change in SD was recorded during the initial profile, which suggests that there was no discrimination between background levels of fluorescent label and the chip substrate.

At approx. 400 s, however, there was a large increase in SD irrespective of background settings, which was most likely due to the onset of coagulation. At this point, samples with background cut-offs of 20 f.u. or greater exhibited sharp, but erratic increases in SD, whereas at 0 and 10 f.u., the profiles were smooth, but less pronounced in terms of rate of change and peak SD achieved.

The changes in SD for the profiles corrected for background above 30 f.u., combined with the absolute fluorescence values obtained in Fig. 3 suggest that the distribution of fluorescent label within the measured area must be changing, becoming reduced in some areas and increased in others and that this phenomenon appears to be associated with the onset of clotting.

In addition, the change in SD became more significant during clotting for profiles at 20 f.u. cut off or more, while at the same time the signal-to-noise ratio was reduced resulting in noisier profiles which, in turn, made CTs more difficult to determine. On the other hand, the change in SD obtained with no background rejection (0 f.u.) was slow and gradual and the first point of



**Fig. 4** Change in SD over time obtained for plasma sample spiked with 0.25 U mL<sup>-1</sup> heparin. Data analysed using LabVIEW software at the minimum signal detection settings of the camera between 0 and 70 f.u.



a change in SD was not well-defined. However, at 10 f.u. cut-off, the initial SD was still quite low, while the change in SD observed during coagulation was quite pronounced and not subject to noise and variability.

The time between the start of the assay and the onset of the large change in SD was suggested to equate with the sample CT and these values were determined from the data shown in Fig. 4. To corroborate this, visual examination of the recorded frames was performed. The time points when the creation of the first fibrin fibres could be visually observed were defined as the CT and compared to the CT values which were taken as the time points of sudden increase in SD (Table 1).

At the minimum signal detection settings of 0 and 10 f.u., CT values could be reliably extracted from the SD profiles in Fig. 4, while CT determination on the basis of profiles at detection minima of 20 f.u. or greater was very difficult or impossible to perform. The visual analysis was used as a correction method indicating a "real" time point for clot initiation. The minimum setting of 0 or 10 f.u. allowed CT determination in a relatively reliable way. Prolongation in CT values was observed with increased heparin concentration for both settings. However, analysis at 10 f.u. correlated best with the values determined by visual observation for all tested heparin concentrations and reflected the onset of clotting in a more reliable way than for 0 f.u. By setting the detection minimum to 10 f.u., areas of very low fluorescence signal were neglected, which included micropillars as the darkest areas. Excluding these regions from the SD analysis yielded more reliable results. Analysis at the minimum signal detection of 10 f.u. allowed reliable and accurate CT determination and therefore, was chosen as an appropriate method for further CT determination.

Thus, it has been shown that the change in the distribution of the fluorescence signal correlated very well with the formation of fibrin fibres as observed visually, and that this could be used as a means of identifying the onset of coagulation in a clotting sample.

### Evaluation of the assay on a glass substrate

In addition to the polymeric (cyclic polyolefin) substrate used for the assay development discussed above, a microstructured glass

substrate was also evaluated for the assay (Fig. 1b). Glass functions as a reference material for the development of coagulation time tests since glass is known to potentiate the intrinsic coagulation process and has been used as the foundation of blood clotting tests since the establishment of the Lee and White test in 1913.<sup>22</sup> Other work has shown that polymeric substrates modified with glass-like surfaces can accelerate coagulation in CT tests.<sup>23</sup>

The redistribution of the fluorescence label during the clotting of a plasma sample supplemented with fluorescently labelled fibrinogen was monitored using fluorescence microscopy on the aPTT-coated glass chips for 710 s. Representative images captured at 100, 280 and 500 s are shown in Fig. 5. The monitored area was initially dark with evenly distributed fluorescence signal (Fig. 5a). The presence of brightly fluorescing formations could be observed in Fig. 5b. Following that an increase in signal intensity was observed but the signal was mostly confined around the micropillars (Fig. 5c). Despite the differences in the platform design, micropillar shape, channel and micropillars dimensions between this platform and the previously used 4Castchip®, a similar trend of the fluorescence signal redistribution as an effect of clotting was observed. The results indicate that our assay is universally applicable to different microfluidic substrate materials.

In order to quantitatively determine the onset of clotting, images were analysed by calculation of a change in mean fluorescence intensity with time and using SD calculations (Fig. 6).

The clotting sample initially showed some short term increase in mean fluorescence intensity. At some point, however, there was an actual decrease in fluorescence intensity, followed once again by a gradual rise. It was not possible to correlate the changes in fluorescence intensity with the clotting process and indicate the onset of clotting on the basis of this result. Thus, the SD of the fluorescence intensity was investigated.

For the first 250 s only small changes in SD were observed. At this stage the signal was uniformly distributed within the monitored area (Fig. 5a). After this period, an increase in SD was observed. This period was associated with the redistribution of the fluorescent label (Fig. 5b) and which, as previously suggested, corresponds to the onset of clotting. A continuous increase in the

**Table 1** CT values for plasma samples containing 0–2 U mL<sup>-1</sup> of heparin obtained by visual analysis and on the basis of the SD response profiles in Fig. 4. (—) refers to a meaningless or indeterminate CT read-out

Heparin concentration/U mL <sup>-1</sup>	CT/s								
	Visual analysis	Minimum of signal detection/f.u.							
		0	10	20	30	40	50	60	70
0	290	290	290	—	—	260	—	—	—
	290	330	300	—	350	—	—	290	—
	280	280	290	—	—	—	—	—	—
0.25	350	350	350	360	370	350	—	—	—
	340	340	340	350	—	—	—	—	—
	400	410	400	—	390	420	—	—	—
0.5	470	470	470	—	—	—	—	—	—
	460	480	480	—	—	—	—	—	—
	470	480	480	480	480	—	480	—	—
1	500	640	640	—	—	640	640	—	470
	500	500	500	510	—	—	—	—	—
	480	490	490	470	—	—	—	—	—
2	560	580	560	480	—	480	500	—	—

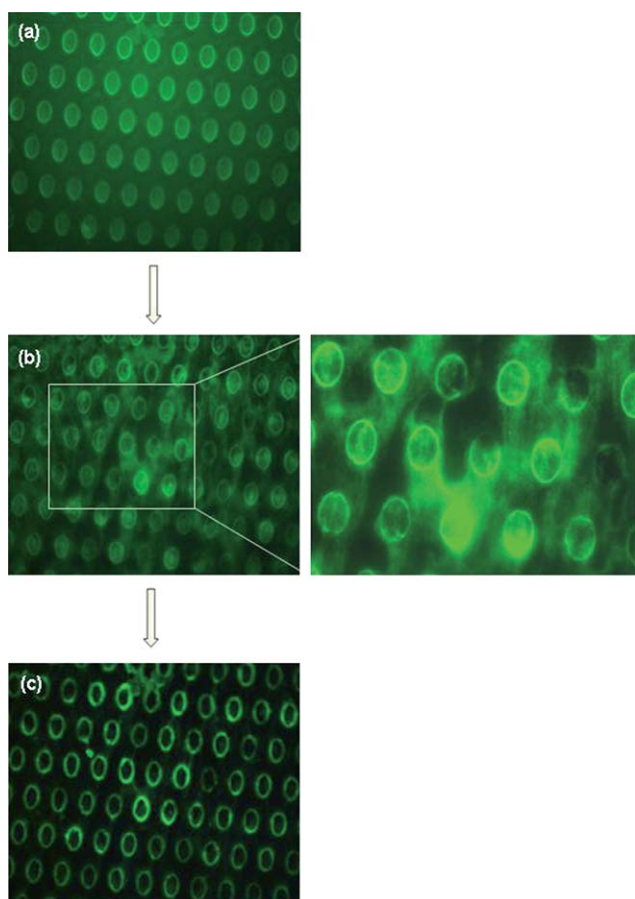


**Fig. 5** Images of the glass micropillar test channel modified with aPTT-SP reagent, containing normal clotting plasma sample supplemented with fluorescently labelled fibrinogen captured using fluorescence microscope with attached video camera at (a) 100 s, (b) 280 s and (c) 500 s after sample application. Magnification used: 10 $\times$ . The inset shows the magnified (20 $\times$ ) localised redistribution of a fluorescence label during clotting.

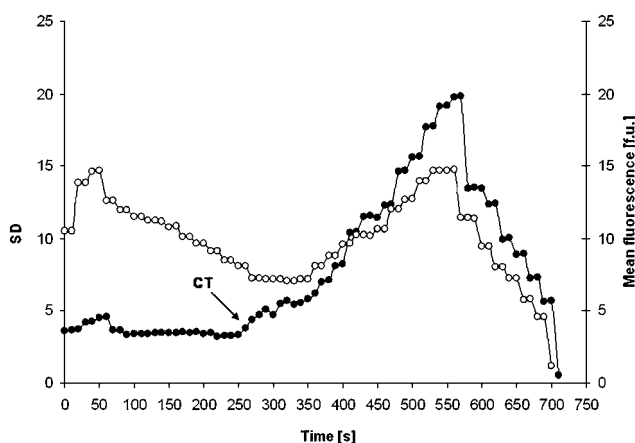


**Fig. 6** Change in the mean fluorescence intensity (open circles) and the SD of the fluorescence intensity (filled circles) over time for a plasma sample supplemented with fluorescently labelled fibrinogen on the glass micropillar channel modified with aPTT-SP reagent. Arrow indicates the time point for the appearance of highly fluorescent regions. Signal measurement interval: 10 s.

SD started at around 350 s. Similar to the previously tested platform, increased localised signal was observed around the pillar, which was most likely an indicator of the onset of evaporation (Fig. 5c). The label accumulation and signal enhancement in the circles around the pillars and decreased intensity in the areas between pillars caused significant changes in the SD, which could be correlated with the appearance of a high peak in SD vs. time profile at approx. 550 s in Fig. 6. Eventually, evaporation seemed to affect areas adjacent to the pillars as well, which could be observed in a gradually decreasing SD signal. As all the liquid evaporated, the fluorescence signal was quenched.

It has been shown that the approach based on the redistribution of the fluorescently labelled fibrinogen during clotting of an activated plasma sample can be successfully utilised to monitor clot formation, localisation and the determination of the clotting initiation on both polymer and glass micropillar substrates. Although the assay was shown to be possible on the glass substrate, further development and optimisation were performed on the polymer-based platform both for the quality of responses and because of the availability of large numbers of chips for assay development.

### Selection of test location

Typical clot monitoring tests were carried out according to the method developed above. The testing took place in the polymer lateral flow platforms coated with 40  $\mu\text{L}$  of aPTT chemistry (SynthASIL). The measurement started with application of a test sample to the sample zone where it came in contact with the dried aPTT chemistry. The whole area of the test channel containing immobilised aPTT reagent became filled with the test sample and was examined in order to select the most appropriate measurement location to monitor clot progression in the most reproducible and reliable manner. Clotting of plasma samples containing 0, 0.25 and 0.5  $\text{U mL}^{-1}$  of heparin was monitored and recorded in areas 1, 2 and 3 as indicated in Fig. 1a.

The collected data were analysed in terms of the SD change over time for normal clotting and heparinised samples monitored in each of the three areas in the channel (Fig. 7). It was shown that the redistribution of fluorescent label was different at zones along the test channel. The CT values for normal and heparinised plasma samples were similar in areas 1 and 2, with the exception of the 0.5  $\text{U mL}^{-1}$  heparin concentration which affected the clotting process so dramatically that there was little (areas 2 and 3) or no (area 1) increase in SD over time, which made the CT calculation impossible. The CTs of the profiles for area 3 were significantly prolonged in comparison to those obtained for areas 1 and 2. There was only a minor increase in SD in area 3 for a normal clotting sample (0  $\text{U mL}^{-1}$  heparin) at around 600 s, which could suggest that the clotting occurred but there was only a limited amount of free fluorescent label available and therefore the signal was very low. A significant change in SD for heparinised samples was observed after more than 1200 s. It was not confirmed if this was due to the occurrence of clotting or some other event. The reason for the low and delayed change in SD recorded in area 3 was not clear. Possibly the portion of plasma that reached the last stages of the journey along the channel could be partly depleted of fibrinogen and/or other coagulation factors which were consumed for clot formation in the early

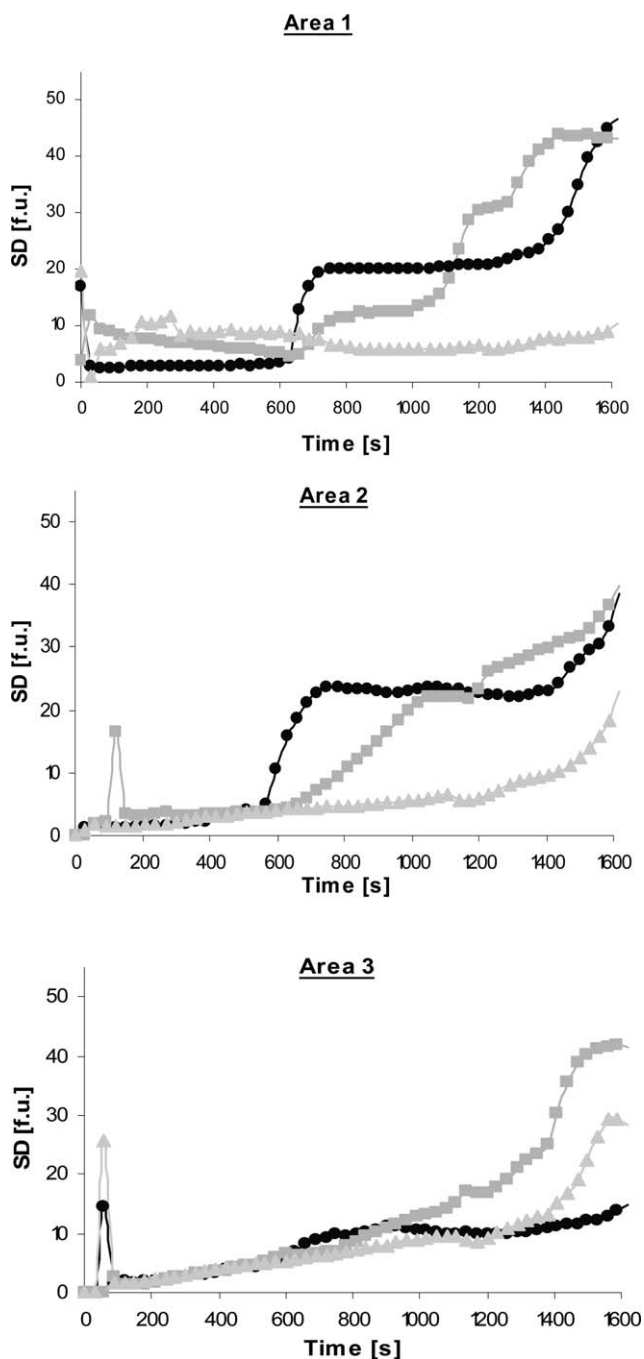


**Fig. 7** Change in SD over time for plasma containing 0 (circles), 0.25 (squares) and 0.5 U mL<sup>-1</sup> (triangles) heparin measured in three areas in the test channel: area 1 representing beginning, area 2, middle and area 3, end of the test channel.

stages of the channel (areas 1 and 2). Alternative explanations could be adsorption of fibrinogen and/or other coagulation factors to the surface, which could have influenced the efficiency and the rate of clot formation in the latter parts of the channel.

An important fact was discovered during visual inspection of the channel filled with clotting solution. The delayed SD increase after 1200 s observed in area 3 might have been simply a result of un-bound, free, labelled fibrinogen accumulating at the end of the channel rather than clotting. The label accumulation could

have brought about an increase in the overall signal, and therefore, overall SD. This could result in a false positive due to the rapid increase in SD which does not correspond to labelled fibrinogen incorporation into the clot, but simply label accumulation.

The profiles obtained for area 2 were clear and distinct in comparison to area 1 where the 0.25 U mL<sup>-1</sup> profile consisted of three steps. Without exhaustive visual analysis it would be impossible to find out which of those three steps corresponded to the initiation of the clotting process. Therefore, area 2 was selected as the most appropriate location for further CT determination.

The absolute CTs were relatively long, being approx. 600 s for normal clotting plasma and longer again for heparinised samples. This may be due to the nature of the aPTT reagent used (SynthASIL) (*i.e.* activity in a dried form, the time required for its release from the surface and physical characteristics of the reagent components such as solubility, *etc.*). It should also be recognised that the developed method is a one-step assay where the contact activation takes place within the test channel and so the time required for the contact activation is included in the total CT value. Therefore, this value does not correspond to the typical aPTT normal CT range given by the manufacturer, which is typically obtained by the standard aPTT procedure that involves a 3 min long pre-incubation step at 37 °C.

#### Effect of evaporation

The potential impact of evaporation on the test was assessed over a prolonged period of time in the polymer lateral flow device, which was not equipped with a lid and therefore was exposed to atmospheric conditions. A standard clotting solution consisting of 1 : 1 mixture of plasma and CaCl<sub>2</sub> supplemented with fluorescently labelled fibrinogen (total volume 25 μL) was applied to the microfluidic platform modified with the aPTT-SP reagent. The percentage loss of mass was measured using a standard laboratory scale and was taken as the evaporation rate (ESI†).

It was shown that the evaporation process was linear under the given conditions for approx. 1500 s (25 min) at which time it reached a plateau and only approx. 6% of the initial sample mass remained. At approx. 780–840 s (13–14 min) 50% of the sample mass had evaporated. Previously observed changes of the fluorescence SD signal due to label relocation were attributed to evaporation, especially for times longer than 780–840 s. It was also established that the first 600 s (10 min) (in the case of a normal clotting sample) was the period that should be monitored, as although 38% of sample mass had been lost, this did not impact on the measurement of coagulation. However, after approx. 780 s (13 min) the measurement was more significantly influenced by evaporation with nearly 50% loss of sample mass and should not be used for CT measurement.

#### Effect of coagulation reagent type

The lateral flow platforms were modified with 40 μL of either Cephalinex, C.K. Prest 2, SynthASIL, aPTT-SP or TriniCLOT aPTT S. Tests were performed on normal plasma and plasma samples spiked with 0.5 U mL<sup>-1</sup> heparin (0.25 U mL<sup>-1</sup> in the case of SynthASIL as 0.5 U mL<sup>-1</sup> prolonged the plasma CT so

drastically that it was impossible to estimate a CT before the sample evaporated). Fig. 8 illustrates the associated clotting profiles obtained for chips modified with these aPTT reagents and Table 2 summarises the extracted CTs obtained for the five tested reagents.

It was difficult to extract the CT values for the samples activated with Cephalinex and C.K. Prest 2 on the basis of the profiles shown in Fig. 8. The change in signal SD was gradual throughout the clotting process and therefore the CTs were not well-defined. However, small inflections in the responses could be observed and so CTs of 360 s and 420 s for Cephalinex and 260 s and 580 s for C.K. Prest 2 were given for normal and heparinised samples, respectively. SynthASIL did show a clear inflection in the SD response and yielded a CT of 600 s for normal clotting plasma, which was nearly two-fold longer than CT achieved with any other tested reagent. High baseline CT values would not be suitable for further assay development, therefore the use of SynthASIL was not considered as an optimal strategy for the assay chemistry formulation. The profiles obtained for aPTT-SP and TriniCLOT aPTT S showed very distinctive changes in SD upon clot formation; the profiles were clear, devoid of noise and thus the CT values were easy to determine for both normal clotting as well as for heparinised samples. However, the delay in clotting due to the addition of heparin was not as significant for

**Table 2** CT values calculated for normal clotting ( $0 \text{ U mL}^{-1}$  heparin) and heparinised ( $0.5 \text{ U mL}^{-1}$  and  $0.25 \text{ U mL}^{-1}$  for SynthASIL) plasma samples tested on platforms modified with dried aPTT reagents

aPTT reagent	CT/s	
	Normal	Heparinised
Cephalinex	360	420
C.K.Prest 2	260	580
aPTT-SP	240	430
TriniCLOT aPTT S	290	370
SynthASIL	600	950

TriniCLOT aPTT S as it was for aPTT-SP. The difference in CT between  $0$  and  $0.5 \text{ U mL}^{-1}$  of heparin was only 80 s for TriniCLOT aPTT S in comparison to 190 s for aPTT-SP. In the case of TriniCLOT aPTT S it would be difficult, if not impossible, to distinguish between  $0$  and  $0.25$  and between  $0.25$  and  $0.5 \text{ U mL}^{-1}$  of heparin in a sample. On the other hand, TriniCLOT aPTT S could be employed in assays for high heparin dosage monitoring (over  $2 \text{ U mL}^{-1}$ ), *i.e.* during surgery. The CT obtained for non-heparinised sample activated with aPTT-SP was the shortest of all the tested reagents (240 s) and addition of  $0.5 \text{ U mL}^{-1}$  of heparin resulted in a significant CT prolongation (430 s). aPTT-SP was thus chosen as the most reliable reagent providing the

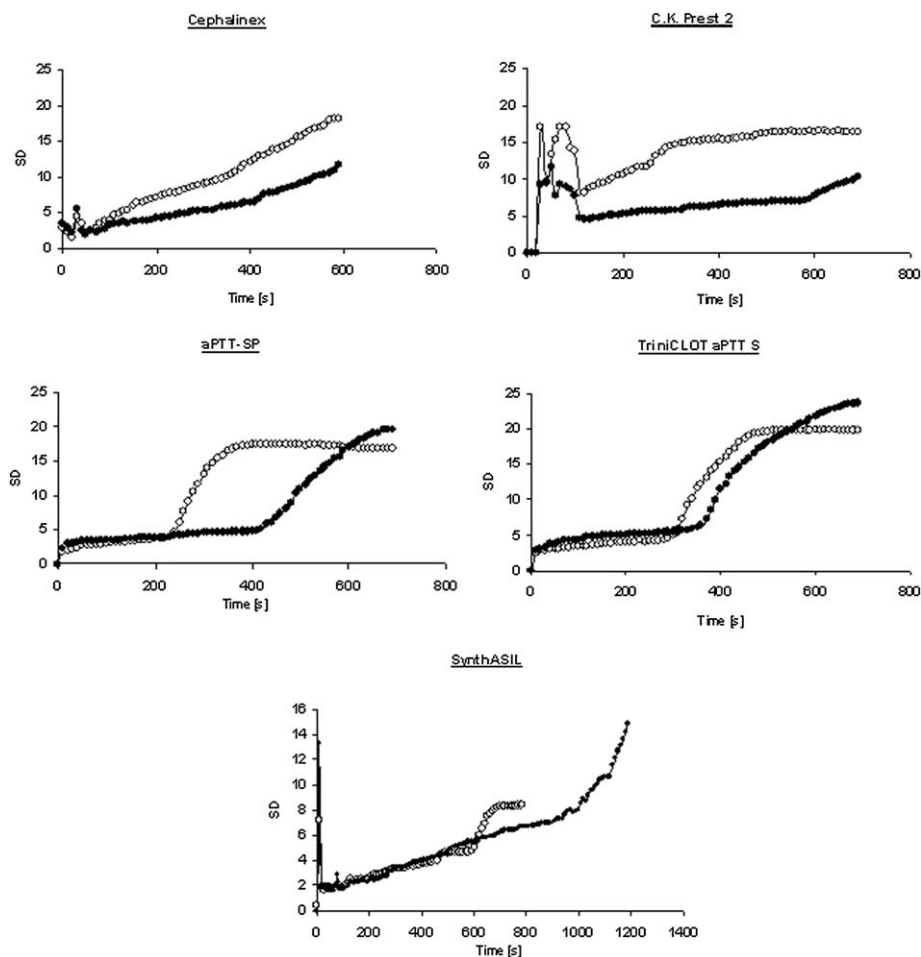


**Fig. 8** Change in fluorescence SD over time obtained for  $0 \text{ U mL}^{-1}$  (open circles) and  $0.5 \text{ U mL}^{-1}$  (or  $0.25 \text{ U mL}^{-1}$  for SynthASIL) (filled circles) heparin in plasma tested on platforms modified with aPTT reagents.



shortest CT and good differentiation between low heparin dose concentrations and was used for further development of the device for monitoring of therapeutic level of anticoagulant (0–2 U mL<sup>-1</sup>).

### Effect of coagulation reagent volume

Typically, a ratio of 1 : 1 of plasma to aPTT reagent in aPTT determination using the tilting tube method or in a plate-based assay is recommended by aPTT formulation manufacturers. The designed device consisted of a channel coated with a dried formulation of aPTT chemistry. Therefore, the ratio of plasma and aPTT could not be equivalent to the ratio in standard assays. The total volume of the test mixture would not be in homogeneous contact with the aPTT chemistry immediately following mixing. Typically, it took 40–60 s for a sample to fill the test channel. Therefore, a study aimed at determining the optimum aPTT reagent volume (and therefore mass) for deposition was performed. 10–50  $\mu$ L of aPTT-SP were drop-coated in the test channel and dried. Regardless of the reagent volume the whole area of the test channel was covered due to capillary filling of the reagent in the channel. Normal clotting (no heparin) and heparinised (0.5 U mL<sup>-1</sup>) samples were tested in duplicate or triplicate.

The SD profiles for 10–50  $\mu$ L of aPTT showed similar trends (ESI†). The change in the SD value was delayed for heparinised plasma in comparison to that of normal clotting plasma for all tested aPTT volumes. The average CTs were between 245–300 s and 400–420 s for normal clotting (0 U mL<sup>-1</sup> heparin) and spiked (0.5 U mL<sup>-1</sup> heparin) plasma samples, respectively. Surprisingly, there was no significant difference in the CTs obtained for plasmas triggered with aPTT deposited at different volumes. Even a five-fold difference in the aPTT reagent volume did not bring about any significant change in the CT value. It has been shown that even low aPTT reagent to plasma ratios were capable of effectively activating the sample. However, significant differences in the quality of the obtained SD vs. time profiles were noticed, which was a significant factor in the CT determination. The use of 10 and 20  $\mu$ L aPTT was shown to generate noisier profiles resulting in less obvious inflections and greater difficulty in CT determination. In comparison, 30 or 40  $\mu$ L profiles were well-defined and CTs could be easily assessed. 50  $\mu$ L was as good as 30 and 40  $\mu$ L. However, such a high volume was difficult to apply. Therefore, 30  $\mu$ L was selected as an optimum volume of an aPTT reagent to be used in the further assay platform development.

### Calibration in heparin-spiked human plasma samples

Following optimisation of the assay with regard to the choice of microstructured platform (polymeric), type of aPTT assay reagent (aPTT-SP), reagent volume (30  $\mu$ L), measurement location (area 2) and the optimal measurement settings for the detection of changes in standard deviation upon clotting (background cut off at 10 f.u.), a calibration was performed using human serum samples spiked with a range of heparin concentrations from 0 to 2 U mL<sup>-1</sup> ( $n = 3$  for all samples except 2 U mL<sup>-1</sup> where  $n = 1$ ). The extracted clotting time responses are shown in Fig. 9. The data show that there is good differentiation

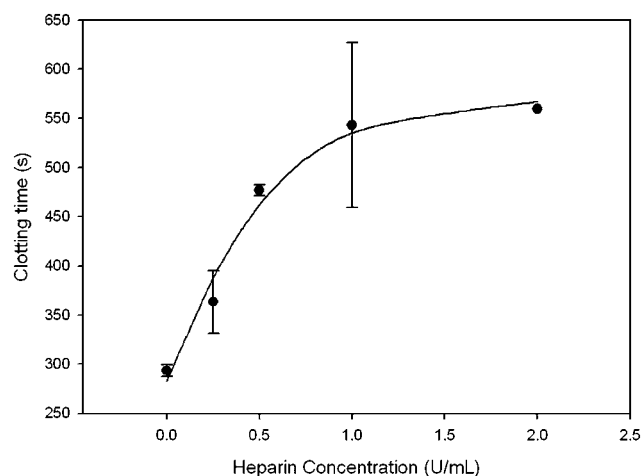


**Fig. 9** Calibration curve showing relationship between the concentration of heparin in spiked human plasma samples and the resulting clotting time extracted from the SD profiles as derived from the fluorescence response of the assay ( $n = 3$  except for 2 U mL<sup>-1</sup> where  $n = 1$ ).

of heparin concentration up to 1.5 U mL<sup>-1</sup>, but the assay begins to plateau at 2 U mL<sup>-1</sup>. This observation is broadly in line with most measures of heparin using aPTT tests which rarely exceed 1 to 1.5 U mL<sup>-1</sup> heparin in spiked samples.<sup>24</sup> The standard deviations were acceptable in all cases except for 1 U mL<sup>-1</sup> heparin. However, it should be noted that as a sample frame is only taken every 10 s, considerable imprecision is introduced into the determination of the clotting time as it can deviate by a minimum of  $\pm 10$  s. Further optimisation of the system to capture data more rapidly may improve this. Nevertheless, the potential for the device to be used to measure aPTT clotting time has been illustrated. This work forms the foundation for further optimisation of the assay for clinical measurement of heparinised blood samples.

### Conclusion

The ability to identify the onset of *in vitro* clot formation using the redistribution of a fluorescently labelled fibrinogen marker was demonstrated. It was shown that in both polymeric and glass microstructured lateral flow device platforms, the fluorescent label becomes redistributed due to its incorporation into the forming clot, which leads to changes in the fluorescence SD over time. These changes were shown to correlate with the formation of fibrin fibres and thus the onset of coagulation. The system was further optimised in terms of the impact of evaporation on the assay, the choice of location for monitoring clot formation and the type and amount of reagent required to bring about activation of the clot in the channel. The platform could be applied to the development of specific assays for monitoring coagulation and the impact of anti-coagulant drugs.

### Acknowledgements

This material is based upon works supported by the Science Foundation Ireland under grant no. 05/CE3/B754. ZHF thanks Science Foundation Ireland for the E.T.S. Walton award.

## References

- 1 M. Hall, A. Noble and S. Smith, *A Foundation for Neonatal Care: A Multi-Disciplinary Guide*, Radcliffe Publishing, 2009.
- 2 A. J. Carter, K. Hicks, A. W. Heldman, J. R. Resar, J. R. Laird, V. J. Coombs, J. A. Brinker and R. S. Blumenthal, *Cathet. Cardiovasc. Diag.*, 1996, **39**, 97–102.
- 3 J. A. Koepke, in *Standardization of Coagulation Assays: an Overview*, ed. D. A. Triplett, College of American Pathologists, 1982.
- 4 J. T. Brandt and D. A. Triplett, *Am. J. Clin. Pathol.*, 1981, **76**, 530–537.
- 5 L. Poller, J. M. Thomson and D. A. Taberner, in *2nd International Symposium on Standardization and Quality Control of Coagulation Tests: Implications for the Clinical Laboratory*, Rome, Italy, 1989, pp. 363–370.
- 6 P. M. Mannucci, in *Standardization of Coagulation Assays: an Overview*, ed. D. A. Triplett, College of American Pathologists, 1982, pp. 165–177.
- 7 E. A. van der Velde and L. Poller, *Thromb. Haemostasis*, 1995, **73**, 73–81.
- 8 G. A. Shapiro, S. W. Huntzinger and J. E. Wilson, *Am. J. Clin. Pathol.*, 1977, **67**, 477–480.
- 9 K. Lo, W. S. Denney and S. L. Diamond, *Pathophysiol. Haemostasis Thromb.*, 2005, **34**, 80–90.
- 10 E. W. Merrill, *US Pat.*, 4884577, 1989.
- 11 G. McMahon, *Analytical Instrumentation: a Guide to Laboratory, Portable and Miniaturized Instruments*, Wiley-Interscience, 2007.
- 12 P. Abgrall and N. T. Nguyen, *Nanofluidics*, Artech House, 2009.
- 13 K. H. Chung, J. W. Hong, D. S. Lee and H. C. Yoon, *Anal. Chim. Acta*, 2007, **585**, 1–10.
- 14 A. A. Saha, S. K. Mitra, M. Tweedie, S. Roy and J. McLaughlin, *Microfluid. Nanofluid.*, 2009, **7**, 451–465.
- 15 S. Thorslund, R. Larsson, J. Bergquist, F. Nikolajeff and J. Sanchez, *Biomed. Microdevices*, 2008, **10**, 851–857.
- 16 M. W. Losey, R. J. Jackman, S. L. Firebaugh, M. A. Schmidt and K. F. Jensen, *J. Microelectromech. Syst.*, 2002, **11**, 709–717.
- 17 S. U. Son, J. H. Seo, Y. H. Choi and S. S. Lee, *Sens. Actuators, A*, 2006, **130**, 267–272.
- 18 M. M. Dudek, T. L. Lindahl and A. J. Killard, *Anal. Chem.*, 2010, **82**, 2029–2035.
- 19 K. W. Ro, H. Liu and D. R. Knapp, *J. Chromatogr., A*, 2006, **1111**, 40–47.
- 20 A. Bhattacharyya and C. M. Klapperich, *Anal. Chem.*, 2006, **78**, 788–792.
- 21 M. M. Dudek, R. P. Gandhiraman, C. Volcke, S. Daniels and A. J. Killard, *Plasma Processes Polym.*, 2009, **6**, 620–630.
- 22 R. I. Lee and P. D. White, *Am. J. Med. Sci.*, 1913, **145**, 495–503.
- 23 M. M. Dudek, R. P. Gandhiraman, C. Volcke, A. A. Cafolla, S. Daniels and A. J. Killard, *Langmuir*, 2009, **25**, 11155–11161.
- 24 A. I. O'Neill, C. McAllister, C. F. Corke and J. D. Parkin, *Anaesth Intensive Care*, 1991, **19**, 592–601.